CHAPTER 69

Wave Group Modulations in Cross-shore Breaking Patterns

T. C. Lippmann[1] and R. A. Holman[2]

ABSTRACT

The principal aim of this work is to quantify the long period (group) time scales associated with incident wave breaking in the surf zone. A video based sampling technique is employed to distinguish those waves which are breaking from those which are not. The technique relies on the gray tone contrast between higher luminance of turbulent generated bubbles and foam associated with wave breaking, and the darker, unbroken surrounding water. Video image intensity time series, $I(x,y,t)$, are sampled across the width of the surf zone at 10 m increments, from just outside the shore break to the far offshore region of the wave breaking. Outside the point of minimum depth (at the bar crest), the width of the surf zone fluctuates over several hundred meters. In this region, low frequency oscillations in I, phase coupled to the crest of breaking incident waves, are associated with wave groups. Cross-shore phase relationships indicate a shoreward progressive group structure up to the crest of the bar. Landward of the bar crest in the trough, low frequencies in I are uncoupled from group modulations seaward of the bar. Video data also show that wave breaking does not cease immediately as waves propagate past the bar crest, but continues well into the deeper water of the trough.

INTRODUCTION

Modulations in wave height of incident sea and swell produce variations in the position of break points in the surf zone. These modulations are on the order of wave groups, with much longer periods than typical gravity waves. In the past two decades, considerable effort has been focused on understanding the importance of wave groupiness inside the surf zone.

[1]Department of Oceanography, Naval Postgraduate School, Monterey, CA 93943

[2]College of Oceanic and Atmospheric Sciences, Oregon State University, Corvallis, OR 97331-5503.

Previous estimates of breaking wave distributions in the surf zone were determined by visually identifying breaking waves in the time series of sea surface elevation on site during the collection of the data (Thornton and Guza, 1983; Whitford and Thornton, 1988). Breaking waves were defined as "when white water was observed passing the sled mast" (Whitford and Thornton, 1988). This method works well, although with tremendous logistical effort.

In this study, video-based data are presented which quantify the temporal evolution of breaking wave patterns on wave group time scales in a cross-shore transect across the width of the surf zone. In our methods, essentially the same determination of breaking waves is utilized but with a higher level of quantification, synchronous ground coverage over large spatial areas, and reduced logistical difficulty. The premise of the technique is based on contrast between the relatively low luminance of non-breaking water and the higher luminance of actively breaking waves and bores. An example snap shot of wave breaking is shown in Figure 1. The high intensity of the foam and bubbles created from active wave breaking contrasts with the darker non-breaking water. Local maxima in image intensity associated with the turbulent water motion of the breaker or roller is phase locked to a region near the crest of the wave (Figure 2).

Our principal aim is to quantify the time scales associated with modulations in incident wave breaking, η_b. We hypothesize that time series of image intensity, $I(x,y,t)$, can be used as a means to quantify the time (and space) scales of $\eta_b(x,y,t)$ at given locations throughout the surf zone. Thus we assume

$$I(x,y,t) \propto \eta_b(x,y,t) \tag{1}$$

where x and y are the cross-shore and alongshore Cartesian coordinates, respectively. For this work we are only interested in the phase relationship and coherence in (1), not the absolute magnitude of I. This relationship has been shown to work well for estimating the phase speed and wave angle of breaking waves (Lippmann and Holman, 1991). An example time series of both I and η_b from the same position in the surf zone is shown in Figure 2 (taken from Lippmann and Holman, 1991). The passage of breaking waves is clearly identified in the video data. There are also waves which are not identified in I, indicating that not all the waves are breaking.

Quantification of images is accomplished using a real time image processing system. Video frames are digitized by the image processor into an array of 512 x 480 picture elements (pixels). Individual pixels store the value of light intensity (luminance) in gray shades from 0 (black) to 255 (white). Images are digitally enhanced to stretch the contrast in the image prior to analysis.

Fig. 1. Example photographic snap shot of wave breaking in the surf zone from October 13, 1990 at ~0900 EST. Breaking waves and bores are identified by the sharp contrast between breaking and non breaking waves.

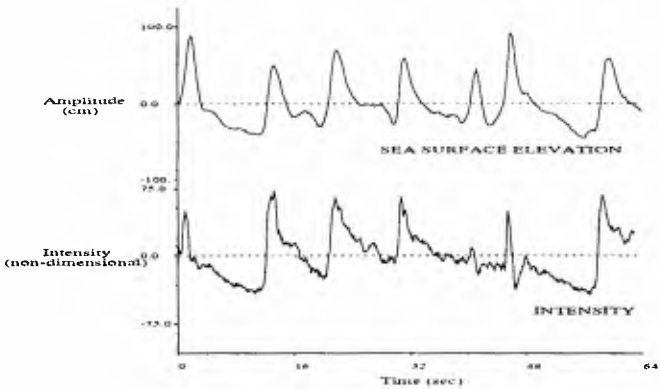

Fig. 2. Example co-located sea surface elevation (converted from pressure data; top) and video image intensity (bottom) mean-corrected time series from October 12, 1990 (from Lippmann and Holman, 1991).

Image locations of interest (for example the location of a fixed surf zone instrument) are determined using known photogrammetric transformation equations assuming the vertical coordinate to be the still water level (Lippmann and Holman, 1989). Time series at each location are then collected by sampling the corresponding pixel intensity at 6 Hz for the entire run (tape) length of ~2 hours. Resolution in image pixels is typically much less than 1 m in the cross-shore direction, and from ~0.5-2.5 m in the longshore direction.

A brief description of the field site and ancillary measurements used in the study is presented next. Analysis of wave breaking time series are then presented as a function of cross-shore distance. Results are then briefly discussed in terms of surf zone forcing models and cross-shore distributions in wave breaking patterns.

FIELD METHODS

The data were collected as part of the DELILAH experiment in October of 1990, held at the Army Corps of Engineers Field Research Facility (FRF) on the Outer Banks of North Carolina near the village of Duck. A general description of the experiment and beach conditions at the FRF is given by Birkemeier, *et al.* (1991). The imaged area ranges from the dune crest to ~400 m offshore and begins ~180 m north of the FRF pier and extends alongshore ~350 m. The cameras were mounted on top of a 44 m high tower in weatherproof housings and hard wired to the FRF building for recording. Video time series were sampled along a cross-shore transect, from just outside the shore break (x = 135 m) to the far reaches of the surf zone (x = 505 m) with a spacing of 10 m.

Data are presented from October 13 at ~0645 EST, coinciding with swell generated by Hurricane Lily. Low tide (-0.21 m NGVD) occurred at ~0900 EST. A photographic snap shot from this day is shown in Figure 1. The offshore incident waves during this period were long crested and energetic, with $H_s \approx 2.23$ m in 8 m depth. Directional spectra from an alongshore array of pressure gages in 8 m depth (Long and Oltman-Shay, 1991) shows a very narrow banded swell at the peak frequency, $f_p \approx 0.083$ Hz, approaching from an incident angle $\alpha_0 \approx 24°$ CW from normal to the beach. The nearshore bathymetry consisted of a prominent linear bar ~100 m offshore (Birkemeier, pers. comm.). Cross-shore profiles at the position of the cross-shore transect from October 12, 13, and 14 are shown in Figures 3 and 5. For reference, the position of the shoreline is at $x \approx 120$ m and the approximate bar crest is at $x \approx 220$ m.

RESULTS

The one-dimensional pattern of wave breaking is shown graphically by plotting together time series of I sampled along a cross-shore transect spanning the width of the surf zone. Figure 3 shows 38 I time series, each of 120 minute duration, stacked vertically with offshore distance increasing toward the top of the figure. Intensity values are normalized to +/- 3 standard deviations about the mean in each respective time series. Also shown on the right hand side is the approximate beach profile.

Seaward of the bar crest wave breaking distributions clearly show the arrival of wave groups, with breaking being more infrequent in the outer surf zone. The groupy modulations are destroyed by breaking in shallower depths. At the bar crest, nearly all of the waves are breaking. Interestingly, bores do not cease breaking immediately landward of the point of minimum depth over the bar, but continue to break well into the deeper water of the trough.

Example auto power spectra (with ~54 degrees of freedom) of I are shown in the upper panels of Figure 4 for locations x = 188 (in the landward slope of the bar) and x = 505 m (in the outer surf zone). Both spectra show a prominent narrow peak at $f \approx 0.08$ Hz, corresponding to the peak incident frequency ($f_p \approx 0.083$ Hz). There is also considerable low frequency variance, as has been observed in previous video time series (Lippmann and Holman, 1991). This low frequency energy occurs at all locations sampled in the surf zone (not shown).

Low Frequency Modulations in Wave Breaking

If modulations in the breaking wave field are associated with wave groups, with periods long compared to peak incident periods, then we expect low frequeney energy in I to be coupled with incident frequencies. Coupling between frequencies in the power spectrum of any given time series are detected with the third order spectrum, the bispectrum (*e.g.*, Kim and Powers, 1979; Elgar and Guza, 1985a). The bispectrum is a measure of lowest order triad interactions between a pair of primary frequencies (f_1, f_2) and a secondary frequency, f_3

$$f_1 \pm f_2 = f_3 \tag{2}$$

Sum interactions in (2) generate harmonics which are phase-locked to the primary, and thus are not free and travel at the phase speed of the primary (Elgar and Guza, 1985b). Difference frequencies are associated with coupling between two signals of nearly the same frequency, and a secondary low frequency signal. In strongly amplitude modulated time series, lower frequency signals are phase-coupled to the primary frequencies, as in rectified signals commonly found in electrical engineering applications.

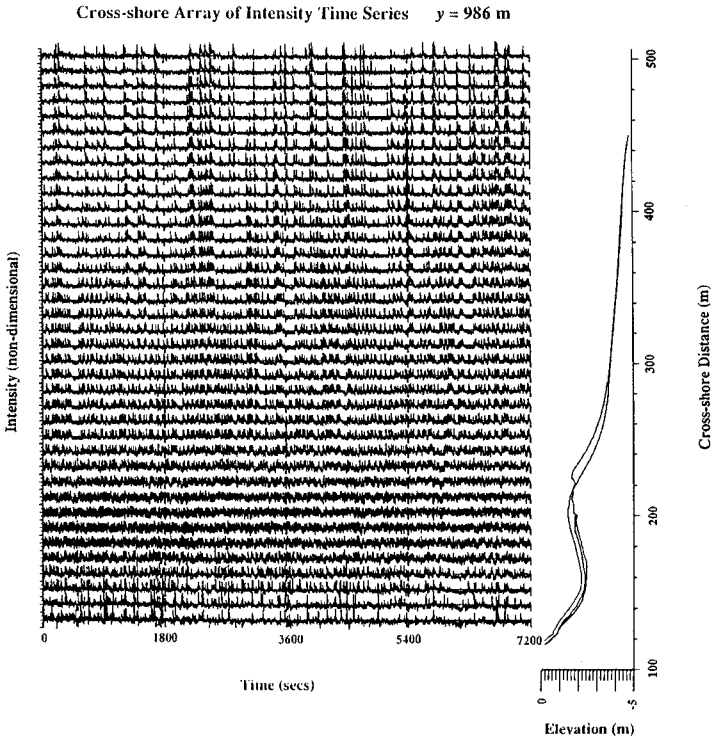

Fig. 3. Time series (120 minute records) of I sampled along a cross-shore transect at 10 m intervals, from just beyond the shore break to the outer surf zone. The vertical axis is nondimensional image intensity (mean corrected) scaled to +/- 3 standard deviations. Time series are stacked vertically with offshore distance increasing toward the top. The beach profile along the transect is shown at the right.

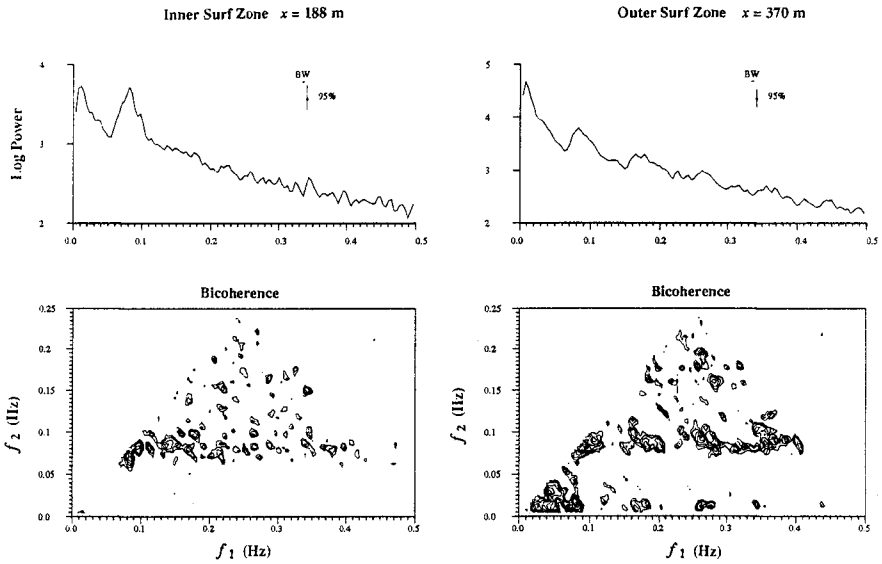

Fig. 4. Example power spectra (upper panels) and bicoherence (lower panels) for I sampled on the landward slope of the bar (left panels) and in the far offshore region of the surf zone (right panels). Bicoherences greater than the 95% significance level for 56 d.o.f. (b = 0.33) are plotted in bi-frequency space with f_1 along the horizontal axis and f_2 along the vertical axis.

Bicoherence (b, normalized bispectrum) estimates from I sampled in the trough of the bar (x = 188 m) and in the outer region of the surf zone (x = 370 m) are shown in the lower panels of Figure 4. Only contours of bicoherence which are greater than the 95% significance level (b_{crit} = 0.33) are plotted (at 0.5 increments). Due to its symmetry properties, only the unique portion of the bispectrum is shown (see Kim and Powers, 1979). Figure 4 shows strong coupling between the primary frequency (0.08 Hz) and the higher harmonics in both regions of the surf zone, arising from the sharp (non sinusoidal) peaks in the time series records. Strongest coupling occurs at the self-self interaction (f_p, f_p), $b \approx 0.61$ and $b \approx 0.68$, and the interaction between the primary and first harmonic (f_p, $2f_p$), $b \approx 0.51$ and $b \approx 0.55$, for the inner and outer surf zone data, respectively.

There is a distinct lack of coupling between incident ($f \geq f_p$) and lower frequencies ($f << f_p$) in the trough of the bar, suggesting that I variance at infragravity frequencies in the trough is derived from free signals not directly associated with incident wave breaking. However, seaward of the bar crest, widespread bicoherence at low f reveals strong coupling to f_p. Highest coupling ($b \approx 0.62$) occurs at (f_1, f_2) $\approx$ (0.082, 0.015). Low frequency spectral energy in I in this region is coupled to modulations in incident wave breaking patterns throughout the surf zone seaward of the bar.

Phase Propagation of Breaking Wave Groups

Wave group modulations also appear coherent across the surf zone up to the region near the bar crest (Figure 3). The phase propagation of the groups can be quantified using frequency domain (complex) empirical orthogonal functions (CEOF). In CEOF analysis, eigenvectors of the cross-spectral matrix are computed at each frequency (Wallace and Dickinson, 1972). Thus the data are decomposed into orthogonal factors representing the amplitudes and phases at each frequency as a function of cross-shore distance.

The first CEOF from the peak incident frequency ($f_p \approx 0.082$ Hz), and also from the low frequency peak ($f \approx 0.015$ Hz) observed in the power spectra (Figure 4) are shown in Figure 5. Only the first factor is shown since it contains the greatest proportion of the variance (63.7% at f_p and 45.9% at low f), and because orthogonality constraints in the decomposition of the data make interpretation of higher modes unclear. CEOF phases are relative to cross-shore position (the absolute value of individual phase estimates is arbitrary), and amplitudes are normalized by the spectral power within each frequency band. Also shown are estimated (relative) phase relationships for phase speeds, C_p, predicted by shallow water (Solitary) wave theory

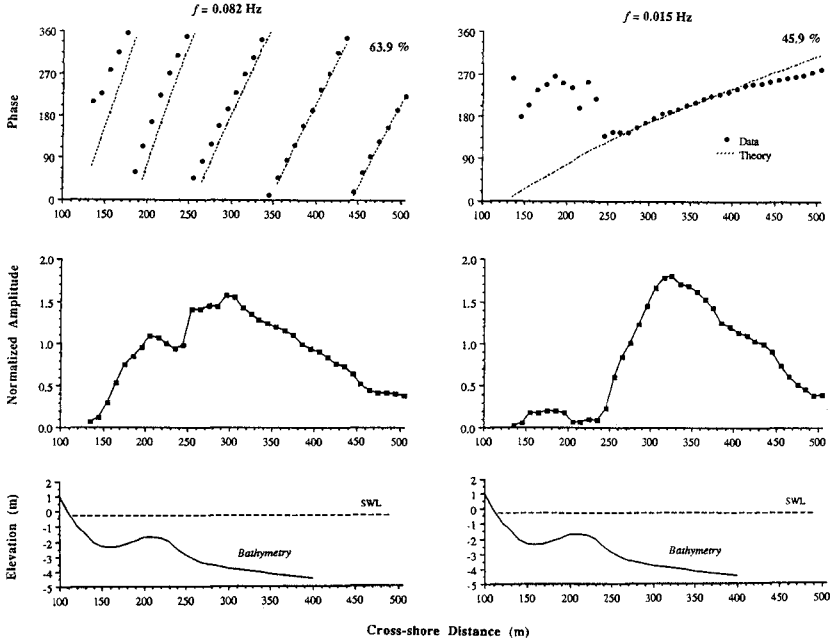

Fig. 5. Frequency domain empirical orthoganal functions (CEOF) from I at the peak frequency (f_p = 0.082 Hz; left panel) and also the low frequency peak in the power spectra (f = 0.015 Hz; right panel), plotted as a function of cross-shore distance. Phases are shown in the upper panels and normalized amplitudes in the middle panels. The approximate (smoothed) beach profile (from October 14) is shown in the lower panels for comparison. Predicted relative phase relationships (equation 4) are indicated with the dashed lines in the phase plots.

$$C_p = \sqrt{g(h + H_{\mathrm{rms}})} \tag{3}$$

where H_{rms} is the root mean square wave height. H_{rms} across the surf zone was estimated using the random wave dissipation model of Thornton and Guza (1983), shown previously to well predict the energy decay of incident wave energy in the surf zone. The predicted phases, $\phi(x)$, in Figure 5 were computed by

$$\phi(x) \approx \frac{2\pi f \Delta x}{\overline{C}_p} \tag{4}$$

where $\overline{C}_p$ is the mean phase speed of the peak incident waves over the distance Δx = 10 m.

For f_p, predicted and observed phases are matched at the most seaward location to allow comparison across the surf zone. The first CEOF shows a clear negative phase ramp, indicating shoreward progressive (breaking) incident waves are coherent all the way through the surf zone. The data are reasonably predicted by (4), although near the bar crest and in the trough the theory systematically over predicts the observations (*i.e.*, steeper phase ramps), consistent with previous comparisons with video derived data (Lippmann and Holman, 1991).

At the low frequency peak ($f \approx 0.015$ Hz), the cross-shore phase structure in the first CEOF also has a linear trend, but only seaward of the bar crest. In this region theoretical group phase speeds are in excellent agreement with the data (although deviates slightly in the far reaches of the surf zone, $x > \sim 425$ m). Predicted phases relationships (4) are best fit to the data in the region of (approximately) constant celerity, between $x \approx 255$-425 m. The average phase speed between x = 255-425 m, $\overline{C}_p \approx 7.3$ m/s, is very nearly the same as predicted by Solitary theory, $\overline{C}_p \approx 7.5$ m/s. The phase relationships are consistent with a shoreward propagating group modulation in the breaking incident wave field traveling at the group velocity of the incident waves. Furthermore, the very small CEOF amplitudes over the bar crest indicate that low frequencies observed in this region are uncoupled to wave groups seaward of the bar, a consequence of widespread breaking over the bar destroying the group structure in the breaking wave field.

DISCUSSION

In the surf zone, break point amplitudes are often taken as a linear proportion of the depth

$$H_b = \gamma h_b \tag{5}$$

where H_b is the height (twice the amplitude) of the breaking wave, h_b is the water depth at the break point, and γ is a constant of O(1) (*e.g.*, Thornton and Guza, 1982). For a plane sloping bottom, $h_b = x_b \tan\beta$, breaking wave amplitudes can be expressed in terms of break point positions. Models based on forcing due to modulations in break point amplitudes can be distinguished by the behavior of γ. In one type (*i.e.*, Foda and Mei, 1981; Schaffer and Svendson, 1988), break point positions are assumed constant, and the group modulations are allowed to progress to the shoreline. Thus, γ in (5) is a temporal function of the amplitude modulation, in which γ is larger for the bigger waves. In the second type (*i.e.*, Symonds, *et al.*, 1982), γ is assumed constant, and break point position is the parameter that fluctuates.

Our data indicates that the initial break points vary over large distances, ranging from far (> 400 m) offshore for the largest waves to near the bar (~100 m offshore) for the smallest waves. Moreover, the group structure is substantially reduced by wave breaking in the inner surf zone, thus restricting group modulations to seaward of the bar. Thus constant γ more accurately describes the data, and is consistent with energy saturation in shallow depths (verified previously with field data; Thornton and Guza, 1982; Sallenger and Holman, 1985).

Wave Breaking in the Trough

Some recent models predicting longshore current profiles, $V(x)$, have been based on the ensemble distribution of incident wave dissipation, $\langle \varepsilon_b(x) \rangle$ (*e.g.*, Thornton and Guza, 1986; Whitford and Thornton, 1988). Incident wave breaking is assumed to decrease shoreward of the bar crest due to increasing depths in the trough. Thus model predictions over barred profiles suggest that longshore currents are strongest on the seaward flank of the bar where maximum incident wave dissipation occurs. However, recent observations of $V(x)$ at Duck suggests that the maximum current often occurs in the trough, in direct conflict with the dissipation models (Whitford and Thornton, 1988; Howd, *et al.*, 1992).

The decay of wave height across a barred profile is well predicted by the model of Thornton and Guza (1983). However, the model assumes implicitly that no time lag exists between the production of turbulent kinetic energy by wave breaking and actual energy dissipation (a point made previously by Roelvink and Stive, 1989; Nairn, *et al.*, 1991). Our observations of wave breaking across the width of the surf zone (Figure 3) indicate that, although the initiation of breaking is confined to depths seaward of the bar, wave breaking does not cease immediately shoreward of the crest, but continues into the trough. The widespread presence of wave "rollers" and bores past the bar crest suggests that advecting turbulence away from the region of highest production over the bar, can be a viable mechanism for transporting momentum into the trough where often the maximum longshore current is observed.

CONCLUSIONS

A video based technique is presented which accurately quantifies temporal modulations in wave breaking across the width of the surf zone. The technique is based on the gray tone (intensity) contrast between the lighter foam and bubbles created by actively breaking waves and bores, and the darker, surrounding non-breaking water. Thus video records of the surf zone contain visible-band time histories of wave breaking patterns. Quantification is accomplished with an image processing system, in which images are digitized at discrete pixels corresponding to defined field coordinates.

Data are presented from a very narrow banded ($f_p \approx 0.083$ Hz), unidirectional day ($\alpha_0 \approx 24°$ CW) during the DELILAH experiment. In addition to energetic incident frequencies associated with the actively breaking incident waves, considerable low frequency variance was observed in all video time series, from the outer portions of the surf zone to the trough of the bar. In the outer surf zone wave breaking at incident frequencies is coupled to low frequency energy, indicating that fluctuations in break point patterns are associated with long period modulations in incident wave amplitudes. Group modulations propagate landward at the phase speed of the incident waves, consistent with simple shoaling expectations.

Finally, we observe the group structure in the wave field to be greatly reduced by breaking in the inner surf zone. All initiation of breaking occurs seaward of the crest, with generally larger waves breaking further offshore and a higher percentage of breaking waves in progressively shallower depths. This suggests that surf zone forcing models which assume a depth dependence on breaking amplitude are more in keeping with the data (*e.g.*, Symonds, *et al.*, 1982). Furthermore, breaking does not cease at the point of minimum depth at the crest, and in fact breaking is widespread in the trough of the bar. This suggests that lateral mixing of momentum across the surf zone, due to the advection of turbulence at the wave front (*e.g.*, Svendsen, 1984, Roelvink and Stive, 1989; Nairn, *et al.*, 1991, and others), could be an important mechanism for modeling longshore currents.

ACKNOWLEDGEMENTS

This work was supported by the Office of Naval Research, Coastal Sciences program under grant number N00014-90-J1118. Additional funding for DELILAH was provided by CERC. Chuck Long computed the frequency-direction spectra. Ed Thornton provided the surf zone instrumentation for DELILAH. Appreciation is given to the hard working staff of the FRF who provided unparalleled support during the experiment. We wish to thank in particular Bill Birkemeier, Kent Hathaway, Todd Walton, and Todd Holland for aiding in the collection of the video data. The late Paul O'Neill was chief engineer for the OSU group, and without his efforts this

work would not have been possible. Over the past few years, Paul was instrumental in the development of all aspects of our video techniques and image analysis. He was a contemporary scientist, creative engineer, and a good friend.

REFERENCES

Birkemeier, W. A., , DELILAH nearshore processes experiment: Data summary, miscellaneous reports, Coastal Eng. Res. Cent., Field Res. Facil., U. S. Army Eng. Waterw. Exp. Sta., Vicksburg, Miss., 1991.

Elgar, S., and R. T. Guza, Observations of bispectra of shoaling surface gravity waves, *J. Fluid Mech.*, 161, 425-448, 1985a.

Elgar, S., and R. T. Guza, Shoaling gravity waves: comparisons between field observations, linear theory, and a nonlinear model, *J. Fluid Mech.*, 158, 47-70, 1985b.

Foda, M. A. and C. C. Mei, Nonlinear excitation of long-trapped waves by a group of short swells, *J. Fluid Mech.*, 111, 319-345, 1981.

Howd, P. A., A. J. Bowen, and R. A. Holman, Edge waves in the presence of strong longshore currents, *J. Geophys. Res.*, 97(C7), 11357-11371, 1992.

Kim, Y. C., and E. J. Powers, Digital bispectral analysis and its applications to nonlinear wave interactions, *IEEE Trans. Plasma Sci.*, PS-7(2), 120-131, 1979.

Lippmann, T. C., and R. A. Holman, Quantification of sand bar morphology: A video technique based on wave dissipation, *J. Geophys. Res.*, 94, 995-1011, 1989.

Lippmann, T. C., and R. A. Holman, Phase speed and angle of breaking waves measured with video techniques, in *Proceedings of Coastal Sediments '91 Specialty Conference*, pp. 542-556, American Society of Civil Engineers, New York, 1991.

Long, C. E., and J. M. Oltman-Shay, Directional characteristics of waves in shallow water, Technical Report CERC-91-, Coastal Eng. Res. Cent., Field Res. Facil., U. S. Army Eng. Waterw. Exp. Sta., Vicksburg, Miss., 1991.

Nairn, R. B., J. A. Roelvink, and H. N. Southgate, Transition zone width and implications for modeling surf zone hydrodynamics, in *Proceedings of the 22nd International Conference on Coastal Engineering*, American Society of Civil Engineers, 68-81, 1991.

Roelvink, J. A., and M. J. F. Stive, Bar-generating cross-shore flow mechanisms on a beach, *J. Geophys. Res.*, 94(C4), 4785-4800, 1989.

Sallenger, A. H., and R. A. Holman, Wave energy saturation on a natural beach of variable slope, *J. Geophys. Res.*, 90(C6), 11939-11944, 1985.

Schaffer, H. A. and I. Svendsen, Surf beat generation on a mild-slope beach, in *Proceedings of the 21st International Conference on Coastal Engineering*, American Society of Civil Engineers, 1058-1072, 1988.

Svendsen, I. A., Wave heights and set-up in a surf zone, *Coastal Engineering*, 8, 303-329, 1984.

Symonds, G., D. A. Huntley, and A. J. Bowen, Two-dimensional surf beat: long wave generation by a time-varying breakpoint, *J. Geophys. Res.*, 87, 492-498, 1982.

Thornton, E. B., and R. T. Guza, Energy saturation and phase speeds measured on a natural beach, *J. Geophys. Res.*, 87, 9499-9508, 1982.

Thornton, E. B., and R. T. Guza, Transformation of wave height distribution, *J. Geophys. Res.*, 88, 5925-5938, 1983.

Thornton, E. B., and R. T. Guza, Surf zone currents and random waves: Field data and models, *J. Phys. Oceanogra.*, 16, 1165-1178, 1986.

Wallace, J. M., and R. E. Dickinson, Empirical orthogonal representation of time series in the frequency domain. Part 1: Theoretical considerations, *J. Applied Meteor.*, 11(6), 887-892, 1972.

Whitford, D. J., and E. B. Thornton, Longshore current forcing at a barred beach, in *Proceedings of the 21st International Conference on Coastal Engineering*, American Society of Civil Engineers, 77-90, 1988.